Environmental Science
Water Research & Technology

ROYAL SOCIETY OF CHEMISTRY

PAPER

View Article Online
View Journal | View Issue

Cite this: *Environ. Sci.: Water Res. Technol.*, 2025, **11**, 2734

Sustainable and low-cost drinking water production *via* electrodialysis by addressing membrane fouling mechanisms to optimize cleaning strategies

Theekshana Malalagama, [abc] Binghui Tian,*[abc] R. M. G. Rajapakse,[abd] Rehan Gunathilake,[abc] Ling Feng [abc] and Min Yang*[abc]

Received 30th May 2025,
Accepted 10th September 2025

DOI: 10.1039/d5ew00498e

rsc.li/es-water

Groundwater is a vital water source, providing drinking water to at least 50% of the world's population and accounting for 43% of water used in irrigation. In Sri Lanka, 39.6% of the population rely on groundwater for drinking purposes, with 72% of this group residing in rural areas. In several of these regions, groundwater quality is affected by geogenic contaminants such as excessive fluoride, hardness, and salinity, which are linked to chronic health issues. These ion-related problems highlight the need for selective separation technologies, with electrodialysis (ED) emerging as a promising and sustainable option. However, membrane fouling and scaling remain significant challenges. This study aims to investigate the mechanisms of membrane fouling and scaling in ED systems and develop effective cleaning strategies to restore membrane performance. The fouling process involves two stages: organic fouling dominant in the initial stages, followed by inorganic scaling. Pearson correlation analysis revealed a strong negative correlation of −0.94 for organic fouling and −0.63 for inorganic fouling. A similar two-stage fouling behavior was also observed in a one-year field experiment conducted in Sri Lanka, further supporting these findings. An integrated acid–base cleaning method was developed, with acidic cleaning effectively removing inorganic scales and alkaline cleaning addressing organic fouling. The acid–base cleaning approach stands out as a sustainable solution to tackle fouling in ED systems, making it suitable for decentralized groundwater treatment in Sri Lanka.

Water impact

Access to clean water remains a challenge in rural Sri Lanka, where communities rely on untreated groundwater. Electrodialysis (ED) offers a sustainable solution, but membrane fouling limits performance. This study investigates fouling mechanisms and proposes a simple acid–alkaline cleaning method. By restoring efficiency and extending lifespan, the approach supports wider ED use in rural water treatment, improving health and sustainability.

1. Introduction

Groundwater serves as a primary drinking water source for nearly half of the global population, with the reliance exceeding 90% in developing countries like Bangladesh. In Sri Lanka, approximately 39.6% of the population depends on groundwater as their primary source of drinking water, with over 72% residing in rural areas. However, groundwater in these regions is often contaminated with geogenic ions such as calcium, magnesium, sodium, and fluoride, which contribute to water hardness and salinity, and pose health risks. The consumption of water containing excessive fluoride leads to significant health issues such as dental and skeletal fluorosis and is also suspected to play a major role in the rising incidence of chronic kidney disease of unknown etiology (CKDu).[1] To address these health concerns, the Sri Lankan government has established groundwater purifying strategies such as numerous reverse osmosis (RO) and a few nanofiltration (NF) water treatment stations in rural areas. RO is an effective technique

[a] *National Engineering Research Center of Industrial Wastewater Detoxication and Resource Recovery, Research Center for Eco-Environmental Sciences, Chinese Academy of Sciences, Beijing 100085, China. E-mail: tianbh@rcees.ac.cn; Tel: +86 10 62928390*
[b] *University of Chinese Academy of Sciences, Beijing 100049, China*
[c] *China-Sri Lanka Joint Research and Demonstration Center for Water Technology, Ministry of Water Supply, Meewathura, Peradeniya 20400, Sri Lanka*
[d] *Department of Chemistry, University of Peradeniya, Peradeniya 20400, Sri Lanka*

for removing contaminants, although it is associated with several drawbacks such as high operational costs, system complexity, and removal of essential minerals, which may lead to deficiencies of essential nutrients. NF, on the other hand, offers partial ion selectivity and is capable of removing hardness and certain levels of fluoride; however, its performance can vary depending on membrane type, feedwater composition, and operating conditions. This highlights an urgent need for more sustainable, affordable, and user-friendly water treatment solutions for rural communities.[2] In this context, electrodialysis (ED) has emerged as a promising alternative, offering advantages such as selective ion removal at a lower cost and simpler operation compared to RO.[3] However, as in all membrane-based water treatment technologies, ED also faces a major challenge: membrane fouling, which is the accumulation of unwanted materials (foulants) on the membrane surface. Fouling can significantly reduce the efficiency and longevity of any system including ED which undermines its sustainability.[4,5]

Fouling of ion-exchange membranes (IEMs) comes in several forms, each with distinct mechanisms and impacts on membrane performance. These include inorganic fouling, organic fouling, colloidal fouling, and biofouling, as identified in previous studies.[5–7] Inorganic fouling occurs when ions such as calcium, magnesium, barium, sulfate, fluoride, and bicarbonate precipitate as insoluble salts, forming scale on the membrane surface. Organic fouling occurs when organic substances such as aromatic compounds, proteins, oils, carbohydrates, humic acids, and anti-foaming agents adhere to the membrane *via* electrostatic and hydrophobic interactions. Colloidal fouling arises from suspended particles, such as colloidal silica, manganese oxide, aluminum oxide, clay minerals, organic colloids, and iron oxide. These particles accumulate on the membrane surface, blocking the diffusion layer and reducing membrane efficiency. Although biofouling has been less studied in ED, it remains a challenge in other membrane processes, often resulting in the growth of microbial colonies on the membrane surface.[5] While substantial research has been conducted on fouling in pressure-driven processes like RO[8–10] and NF,[11–13] studies focusing on fouling in ED, particularly for groundwater treatment, are relatively limited.

Understanding the mechanisms of membrane fouling in ED and developing effective cleaning strategies are crucial for advancing the sustainability of this technology. Regular cleaning is essential to mitigate fouling and maintain the long-term performance of ED systems, particularly in field applications requiring continuous operation. This study investigates membrane fouling in an ED system treating real groundwater at the laboratory scale, with a focus on understanding the mechanisms of fouling and scaling in Sri Lankan groundwater. The findings were further validated using performance data from a long-term ED plant operated for groundwater treatment. Additionally, it aims to develop and evaluate cleaning procedures to mitigate fouling and restore membrane performance, contributing to more sustainable ED operations. A variety of analytical techniques are utilized to systematically examine membrane morphology, elemental distribution, foulant composition, and scale formation. The effectiveness of chemical cleaning methods in removing foulants and scaling will also be assessed, with the ultimate goal of establishing an optimized cleaning protocol for ED systems in field applications.

2. Materials and methods

2.1. Materials

The ED membranes were intentionally fouled using a batch-type ED unit manufactured by Hefei ChemJoy Polymer Materials Co. in China. The brackish water (water quality characteristics are provided in the SI, Section S1) utilized in these experiments was obtained from a deep well located at coordinates 80.634211, 7.930596 in Kithulhitiyawa, Anuradhapura, Sri Lanka, in March 2023.

Both the dilute and the concentrated chambers were supplied with brackish water sourced from a deep groundwater well. Operational conditions were maintained at higher applied currents and higher flow rates to mimic the conditions intended for implementation in Sri Lankan context for the selective removal of problematic ions such as fluoride and hardness. The initial volume for all three input solutions used was 1000 mL in each batch. During the intermittent desalination experiments, each desalination cycle was conducted for one hour, and the process was repeated until a total of 100 cycles was completed (Fig. S2). A multi-parameter portable meter (HANNA instruments: H198129 Combo pH and EC meter) was used to monitor pH and EC variation in both dilute and concentrate solutions.

2.2. Membrane cleaning

Upon completion of the desalination process, the ED setup was dismantled, and the membranes were retrieved for cleaning. Visual inspection revealed areas of the membrane with most severe damage has the highest concentration of surface fouling. These sections were cut into samples measuring 5.0 cm × 5.0 cm. One sample, retaining all fouling materials, was designated as the original reference sample and the other four samples were subjected to physical and chemical cleaning processes. The cleaning agents used were (I) distilled water (DW), (II) a base solution (NaOH, pH 12), (III) a strong acid (HCl, pH 2.5), and (IV) a weak acid (acetic acid, HAc, pH 2.5). Cleaning was conducted by soaking the different membrane pieces (~0.5 × 0.5 cm^2 each) separately in 100 mL of their respective cleaning solutions while stirring continuously for 24 hours. After soaking, the membranes were removed from the solutions, dried in a desiccator, and prepared for further analysis.

2.3. Analytical methods

2.3.1. Calculations. The desalination efficiency of each batch was calculated using eqn (1), where σ_1 and σ_t are the initial and final values of the feed solution at times $t = 0$ and $t = t$, respectively.[14]

$$D = \frac{\sigma_1 - \sigma_t}{\sigma_1} \quad (1)$$

Eqn (2) was used to calculate the water production rate φ (%), where V_f is the volume of feed (m^3) and V_d is the volume of dilute produced (m^3).[14]

$$\varphi = \frac{V_d}{V_f} \times 100\% \quad (2)$$

The rate of change in removal efficiency of organic and inorganic components between each sampling interval was calculated to characterize the fouling progression. The rate of change of each parameter was calculated using eqn (3).[15]

$$\text{Rate of change} = \frac{\text{value of the parameter at a latter time point} - \text{value of the parameter at an earlier time point}}{\text{Time interval}} \quad (3)$$

2.3.2. Water quality characterization. Basic parameters such as temperature, pH, EC, and TDS were measured onsite using a HANNA multiparameter portable meter (H198129 Combo pH and electrical conductivity meter). The titration method was then used to measure alkalinity and total hardness, following APHA (1998) guidelines. Ion chromatography (Metrohm 930 Compact IC Flex 1, Metrohm AG, Switzerland) was utilized to measure anion concentrations after filtering the water through disposable 0.45 μm membrane syringe filters. Using a TOC analyzer (LCPH/CPN, Shimadzu, Kyoto, Japan), DOC was measured. A UV-visible (UV-vis) spectrophotometer (UV-2600, Shimadzu, Tokyo, Japan) was used to assess the level of organic matter contamination in the water. Organic matter was also analyzed using a three-dimensional fluorescence excitation–emission matrix analyzer (3D-EEM, F-7000, Hitachi, Tokyo, Japan).

2.3.3. Membrane characterization

(1) Scanning electron microscopy (SEM) and field emission scanning microscopy (FE-SEM) studies. The bulk deposits and the structural morphology of the fouled membranes were examined using field emission scanning electron microscopy (FE-SEM, Hitachi SU8020, Hitachi, Japan). Elemental composition was analyzed using a Hitachi S-3000N scanning electron microscope (SEM, Hitachi, Japan) equipped with an energy-dispersive X-ray spectrometer (EDS), while the elemental distribution was assessed using EDS mapping mode. Prior to SEM analysis, the samples were coated with silver nanoparticles to enhance imaging quality.

(2) ATR-FTIR spectroscopy studies. Attenuated total reflectance Fourier-transform infrared (ATR-FTIR) spectroscopy was used to identify the functional groups present in the foulant molecules using a Thermo Scientific Nicolet iS5 FTIR spectrometer. The FTIR spectra were recorded in the range of 4000 to 400 cm^{-1} at a resolution of 2 cm^{-1} with 128 scans per sample point.

(3) X-ray diffraction (XRD). The crystallinity of the IEMs was investigated using X-ray diffraction (XRD) analysis, performed on a MiniFlex600 instrument manufactured by Rigaku, Japan. The XRD analysis utilized Cu Kα radiation of wavelength 1.5406 Å at 40 kV and a current of 40 mA. Diffraction patterns were recorded over a 2θ range, with a scan rate of 5° per minute.

(4) X-ray photoelectron spectroscopy (XPS). XPS analysis was conducted using an ESCALAB 250Xi system (Thermo Fisher Scientific, USA) to determine the elemental composition and chemical states of the fouling deposits. The measurements were carried out with a monochromatic Al Kα source (1486.6 eV). A charge neutralizer was applied to minimize surface charging, and the binding energy scale was calibrated using the C 1s peak at 284.6 eV, which corresponds to aliphatic carbon. The pressure in the analysis chamber was maintained below 2×10^{-6} Pa. Survey scans were acquired over a binding energy range from −10 to 1351 eV, using a step size of 0.5 eV. Additionally, high-resolution scans with a resolution of 0.1 eV were performed for elements such as C 1s, O 1s, Ca 2p, Mg 1s, and S 2p; for detailed analysis, an even finer resolution of 0.05 eV was applied where appropriate.

(5) Statistical analysis. To evaluate the individual and combined effects of organic and inorganic fouling on overall membrane fouling, multiple linear regression analysis was applied. Principal component analysis (PCA) was conducted using SPSS Statistics 25.0, performed separately on ATR-FTIR and EDS datasets to reduce dimensionality and identify representative fouling indicators. For ATR-FTIR, absorbance peaks at 3301 cm^{-1} (–OH), 1670 cm^{-1} (amide I), 1642 cm^{-1} (amide II), and 1246 cm^{-1} (sulfonate) were included. The first principal component, which explained 98.7% of the variance, was strongly correlated with protein- and polysaccharide-related peaks, and was thus interpreted as the organic fouling factor (Org). For EDS, silicon (Si) and calcium (Ca) counts were analyzed, with the first principal component (explaining 95.2% of the variance) representing inorganic fouling (Inorg).[15] The component loadings and eigenvalues confirmed that Org and Inorg captured the dominant variation in the datasets. These two composite variables were then used as independent predictors in regression analysis to evaluate their combined impact on removal efficiency.

2.4. Pilot plant test

A pilot-scale ED experiment was conducted in Kithulhitiyawa, Anuradhapura, Sri Lanka (latitude 7.930596, longitude 80.634211), over a one-year period beginning in September 2023 due to its heavy reliance on groundwater for drinking purposes and its vulnerability to geogenic contamination.

The ED system employed for the pilot experiment was identical to the laboratory setup described in section 2.1, ensuring consistency between controlled laboratory conditions and real-world field operations.

3. Results and discussion

3.1. Electrodialysis performance

Fig. 1 illustrates the performance of the ED plant over 100 operational cycles, highlighting its substantial water production capacity, which exceeds 87% during groundwater desalination. In the initial setup, the system demonstrated high electrical conductivity (EC) removal efficiencies, delivering high-quality treated water. However, as the operation progressed through 100 cycles, a noticeable decline in performance was observed, particularly compared to water quality in the early stages. Fig. 1(a) presents the water production rate as a function of the number of cycles, while Fig. 1(b) depicts the variation in electrical conductivity during intermittent ED tests.

As shown in Fig. 1(a), the water production rate gradually, though slowly, declined over the measured 100 cycles. This reduction in performance can be attributed to several factors, including membrane fouling and scaling.[16] Fouling primarily occurs on the membrane's surface and within its pores due to concentration polarization, while scaling predominantly occurred during intermittent system shutdowns. The presence of scale deposits on the membrane's surface and pores can alter membrane hydrophilicity, facilitating the easier passage of water through the membrane.

The EC in the water produced after 38 cycles remained below 679 μS cm^{-1}, signifying a degradation in water quality with increasing treatment cycles. During the first 21 cycles, EC removal efficiency remained high, ranging from 97.06% to 70.3%, with only a slight decline. However, a sharp drop in efficiency was observed over a few cycles, leading to a significant 30% reduction compared to the initial 21 cycles. This sudden decrease indicates the onset of membrane fouling in the system, a trend that is consistent with the findings of Zhang W. *et al.* in 2022.[17] Following this decline, the efficiency appeared to stabilize, showing alternating periods of decrease and increase. This behavior can be attributed to the ongoing processes of membrane fouling and scaling. During the initial cycles, the IEMs were likely free of significant foulants, allowing efficient ion transport. However, as the cycles progressed, foulants and scale gradually built up on the membrane surfaces, restricting ion movement and reducing performance. This accumulation over time caused a notable drop in EC reduction efficiency, emphasizing the challenges of continuous operation and the importance of implementing effective fouling control strategies.

3.2. Visual inspection of the fouled membrane

A visual inspection encompassed examinations of the system's inlets, outlets, electrodes, spacers, and membranes. This thorough assessment aimed to detect any physical deformations caused by pressure; however, no such deformations were observed, affirming the absence of pressure-induced changes within the system. A more detailed evaluation was conducted on the membrane sheets individually, following the complete disassembly of the ED setup.

AEMs were covered by a distinct, brown-colored layer (Fig. 2a), whereas this layer was comparatively less pronounced on the CEMs (Fig. 2d). This discoloration is attributed to the deposition of humic substances, which are the predominant components of natural organic matter (NOM) and are typically classified as humic acid (HA), fulvic acid (FA), and humin. Although CEMs exhibited less severe coloration than AEMs, the accumulation of reddish-brown contaminants was still observed, albeit at a lower intensity. Similar findings of relatively reduced fouling in CEMs have been reported in

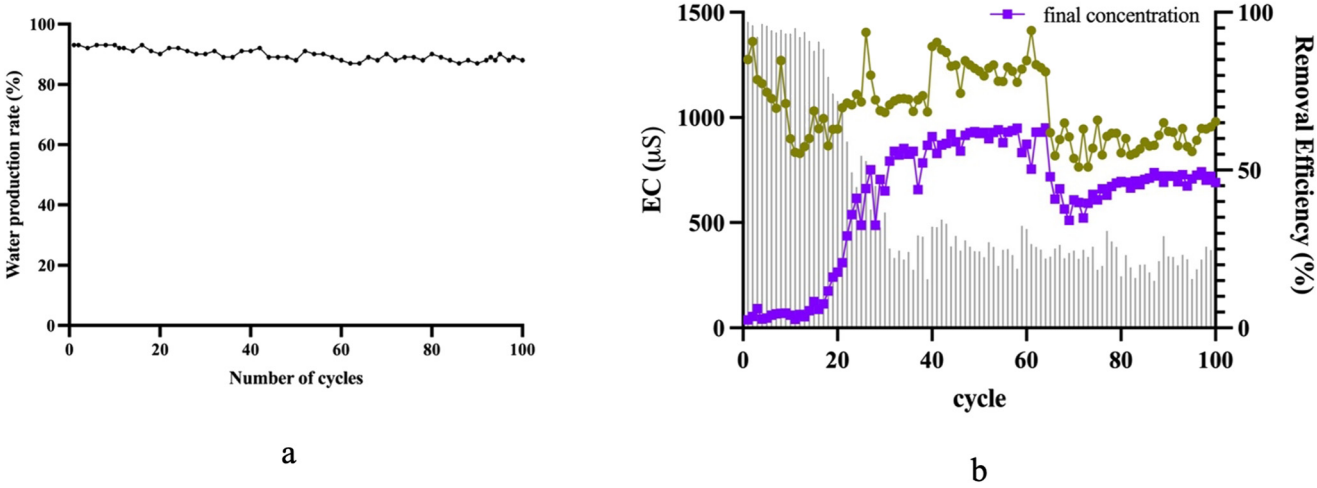

Fig. 1 (a) Water production rate (%) and (b) variation and reduction of electrical conductivity of ED during intermittent ED testing.

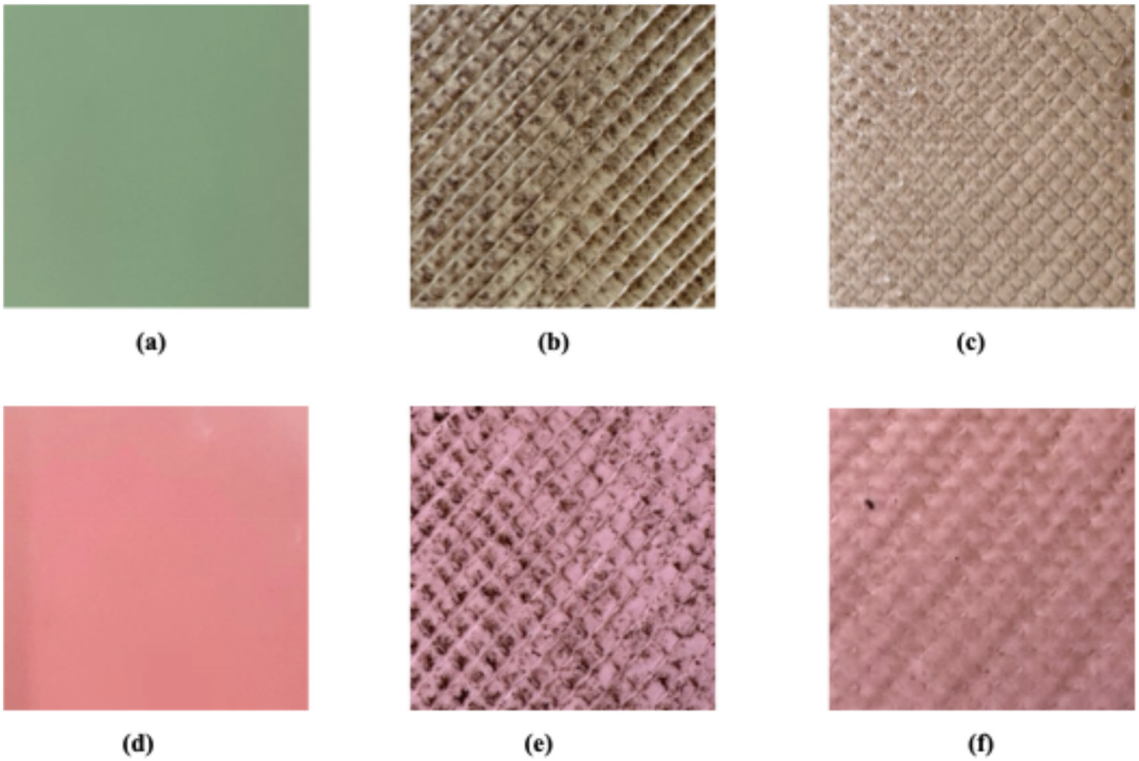

Fig. 2 Photographs of (a) virgin, (b) fouled diluted side, and (c) fouled concentrated side elements of the AEM and (d) virgin, (e) fouled diluted side, and (f) fouled concentrated side elements of the CEM obtained after visual inspection.

previous studies.[18–20] According to these studies, the morphology of fouling appeared similar in both AEMs and CEMs, although the extent differed. Based on these observations, our subsequent analysis primarily focuses on fouling behavior in AEMs.

Fig. 2(a–c) presents a series of images depicting the fouled AEM sheets alongside images of the pristine, untouched AEMs, offering valuable insights into the fouling that occurred on the membranes. The AEM exhibits distinct brown and dark brown colorations, forming well-defined blocks attributed to the creation of water channels across the membrane, demarcated by the spacers. On the outer surfaces of AEMs, which are exposed to the concentrated solution circulation during the ED operation, a thinner layer of fouling is apparent (Fig. 2(c)). A similar fouling pattern was reported by Xia *et al.*, 2018.[21] It is worth noting that IEMs did not exhibit a slimy or gelatinous texture, suggesting that the membrane was not significantly affected by biofouling.

3.3. Fouling morphology and composition of IEMs

The fouled IEMs in the ED system exhibited distinct morphological and compositional characteristics. SEM images reveal that the membrane surfaces are entirely covered by a thick fouling layer (Fig. 3(b)), particularly in the anion exchange membranes (AEMs), where fouling has reached a thickness of

Fig. 3 SEM images of (a) virgin, (b) fouled diluted side, and (c) fouled concentrated side of AEM.

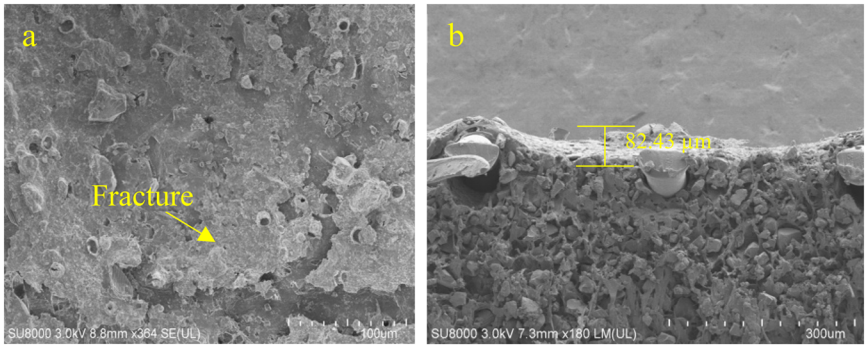

Fig. 4 SEM image of a fouled AEM (a) surface and (b) cross section.

82.43 μm. The fouling materials displayed diverse morphologies, including spherical crystallized formations, needle-like crystals, and block crystals (Fig. 4).

The predominant components of the fouling layer are calcium (Ca) and magnesium (Mg), with both elements forming significant scale deposits. EDS confirms the presence of Ca and Mg, which are primarily identified as calcium carbonate ($CaCO_3$) and magnesium carbonate ($MgCO_3$), respectively (section 2.1 in the SI). XRD analysis further identified multiple crystalline phases of $CaCO_3$, including calcite, vaterite, and aragonite as well as crystalline $MgCO_3$, providing a detailed picture of the scaling (section 2.2 in the SI). Silica (Si) was also a major contributor, with silicon dioxide (SiO_2) present in significant quantities. XPS confirmed the presence of S–O bonds, indicating that silica is a dominant foulant, likely originating from the groundwater (section 2.4 in the SI). Furthermore, organic fouling is observed through FTIR spectroscopy, which detects characteristic bands associated with organic compounds, particularly proteins and polysaccharides (section 2.3 in the SI). These organic foulants are found to be adhered to the membrane surface, contributing to the overall fouling composition. An *et al.* (2023)[22] also reported that low molecular weight (LMW) organic matter tends to accumulate more readily on membrane fouling where significant concentrations of LMW organic compounds are found in raw water (Fig. S1) due to the unique nature of Sri Lankan groundwater.

3.4. Proposed fouling mechanism for IEMs

3.4.1. Identification of fouling mechanism in brackish groundwater treatment using ED technology. This section explores removal efficiency trends, FTIR absorbance data as a marker of organic fouling, and EDS elemental composition as a marker of inorganic fouling. These analyses, complemented by rate-of-change assessments and correlation studies, aim to elucidate the fouling mechanisms in the ED membrane system.

- *Decline in removal efficiency.* The removal efficiency of the ED membrane decreased significantly over the 100-cycle study period, suggesting a progressive decline in membrane performance due to fouling. Initially, at cycle 20, removal efficiency was 71.99%, dropping sharply to 36.52% by cycle 30 and further to 29.59% by cycle 100 (Fig. 1). This trend of

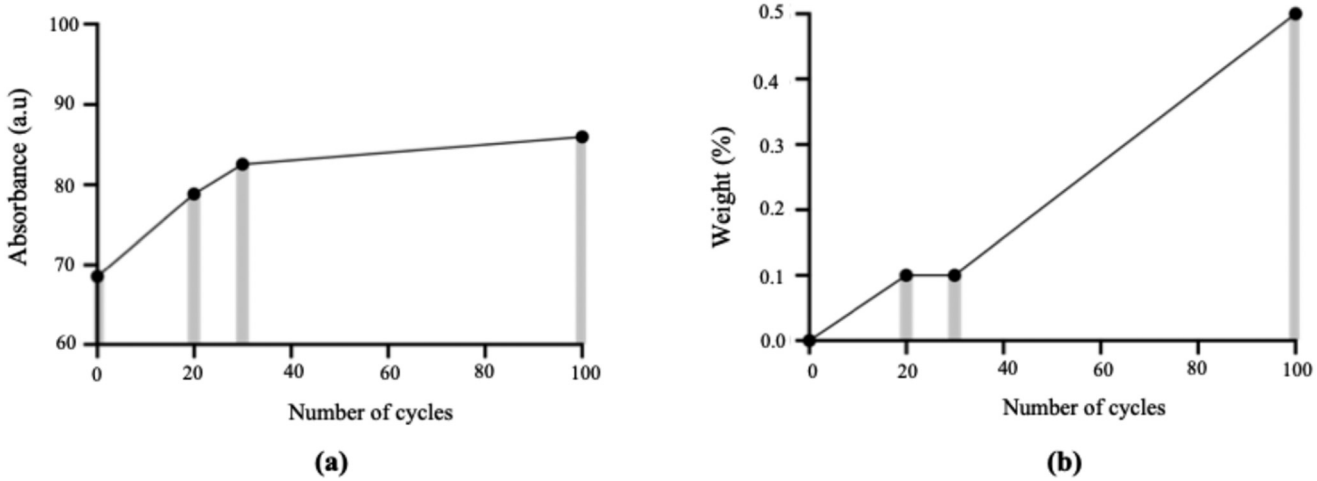

Fig. 5 FTIR absorbance values at 1670 cm^{-1} over time, indicating the progression of organic fouling (a) and EDS elemental composition analysis showing calcium weight % on the membrane over time (b).

rapid fouling during the initial phase of operation was followed by a more gradual decline.

• *Evidence of organic and inorganic fouling.* Fig. 5 illustrates the two-stage fouling mechanism identified during lab-scale ED operation, as observed through FTIR (for organic foulants, Fig. 5(a)) and EDS analysis (for inorganic scaling, Fig. 5(b)), offering valuable insights into the mechanisms of both organic and inorganic fouling.

As shown in Fig. 5(a), organic fouling is quantified using FTIR-based principal component analysis (PC1), which explained 98.7% of the spectral variance. The dominant loadings in PC1 were associated with amide functional groups (1670 cm^{-1}), indicating proteinaceous or organic material accumulation. Organic fouling increased rapidly in the early treatment cycles: absorbance rose from 78.85 at cycle 20 to 85.97 by cycle 100. The highest rate of increase was between cycles 20 and 30. During this period, the rate of change in absorbance was calculated at 0.369 absorbance units per cycle, suggesting a rapid initial fouling stage. After cycle 30, the fouling rate slowed to 0.049 absorbance units per cycle, indicating a near-steady-state phase. This behavior is consistent with stage 1 fouling, where a thin organic layer forms quickly and then stabilizes, reducing membrane performance by obstructing ion transport.

Fig. 5(b) presents the progression of inorganic fouling, as measured by energy-dispersive spectroscopy (EDS). The first principal component (explaining 95.2% of the variance) showed strong loadings for calcium (Ca), confirming the role of calcium-based scaling. During early operation (cycles 20 and 30), calcium deposition remained low at 0.1 wt%, and the rate of change was negligible. However, a gradual but steady increase in Ca content was observed between cycle 30 and 100, reaching 0.5 wt% at cycle 100, with a corresponding deposition rate of 0.0057 wt% per cycle. This trend indicates the onset of stage 2 fouling, where the pre-established organic layer likely promotes the nucleation and growth of inorganic scale (*e.g.*, $CaCO_3$).

These two datasets together support a sequential fouling model:

Stage 1: early organic accumulation driven by electrostatic and hydrophobic interactions.

Stage 2: later-stage inorganic scaling facilitated by the organic layer and operating conditions.

Although the proposed two-stage fouling model is based on post-operation analysis of lab-scale membranes and is not predictive in real time, it offers a valuable mechanistic foundation for understanding fouling progression. To enable early-stage identification during ED operation, future work should incorporate real-time monitoring tools—such as resistance tracking, voltage fluctuations, or current efficiency trends—as potential operational indicators. These could be further enhanced by advanced electrochemical signal monitoring techniques, as demonstrated by Zhang *et al.* (2024),[23] which show strong potential for early detection and differentiation of fouling stages.

Future studies should aim to validate this two-stage fouling model in pilot-scale ED systems, integrating online monitoring tools (*e.g.*, EIS) to enable real-time identification and mitigation of both organic and inorganic fouling stages.

• *Correlation analysis: supporting the two-stage fouling model.* To validate the two-stage fouling hypothesis, Pearson correlation analysis was conducted to evaluate the relationships between removal efficiency and both organic and inorganic fouling. The correlation coefficient between removal efficiency and FTIR absorbance count was $r = -0.94$, indicating a strong negative correlation. This result suggests that increased organic fouling, as measured by FTIR, is closely associated with a significant decline in removal efficiency. This supports the hypothesis that organic fouling is the dominant mechanism driving performance degradation during the early phase of ED operation.

In contrast, the correlation coefficient between removal efficiency and inorganic fouling, as indicated by calcium deposition, is $r = -0.63$, reflecting a moderate negative correlation. This finding indicates that while inorganic fouling also contributes to the reduction in removal efficiency, its impact is less pronounced in the early stages and becomes more significant in later stages of operation. The moderate correlation reinforces the concept of a secondary fouling mechanism, where inorganic scaling gradually accumulates over time, particularly after organic fouling stabilizes. A summary of the Pearson correlation coefficients is provided in Table 1.

A detailed evaluation of removal efficiency, fouling dynamics, rate-of-change calculations, and correlation analysis supports a two-stage fouling model in electrodialysis:

Stage 1 (early phase): organic fouling dominates. This is evident from the sharp increase in FTIR absorbance and its strong negative correlation with removal efficiency. The rapid accumulation of organic deposits significantly impacts membrane performance, with the most noticeable decline occurring within the first 30 cycles.

Stage 2 (later phase): inorganic fouling, particularly calcium scaling, becomes more prominent. This is reflected in a gradual rise in calcium content and a moderate negative correlation between calcium deposition and removal efficiency. Unlike organic fouling, which causes a rapid drop in performance, the effects of inorganic scaling exert a cumulative and slower effect, contributing to a continued but more gradual decline in system performance.

These findings highlight the distinct phases of fouling in ED (Fig. 6) and emphasize the need for targeted mitigation strategies to maintain system performance.

Table 1 Pearson correlation coefficients between removal efficiency and fouling indicators

Correlation pair	Correlation coefficient (r)
Removal efficiency *vs.* organic fouling	−0.94
Removal efficiency *vs.* inorganic fouling	−0.63

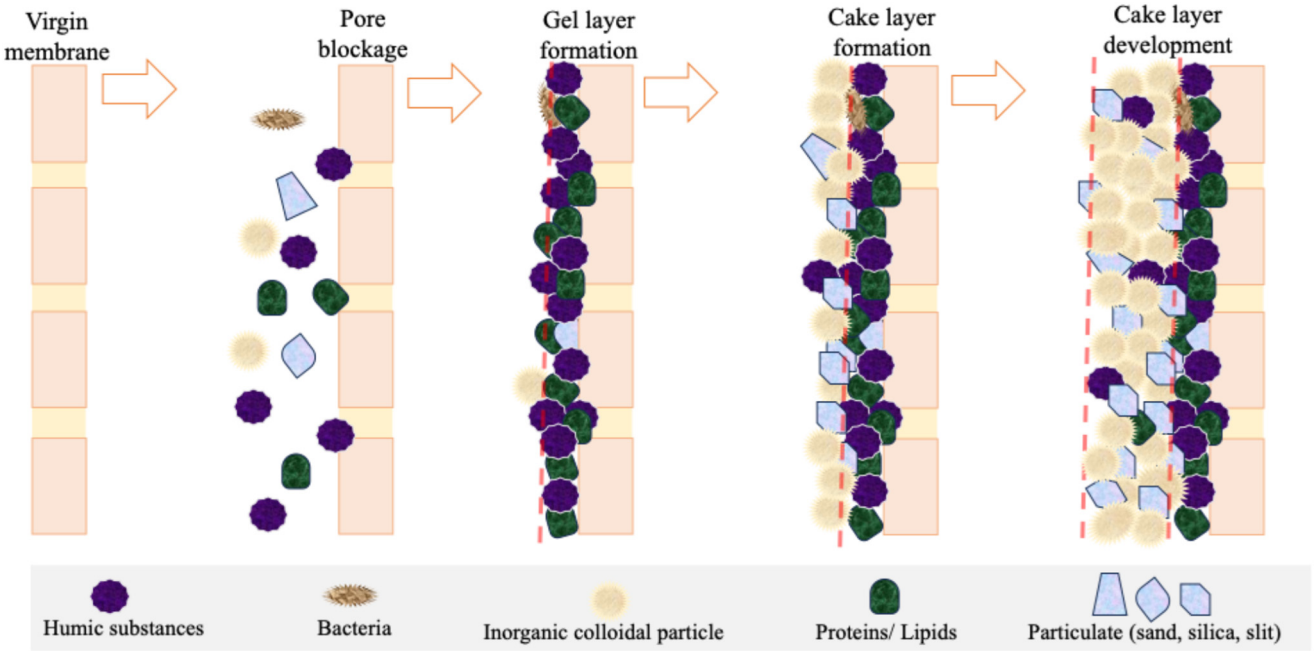

Fig. 6 Schematic diagram to illustrate two-stage fouling occurring in the ED process.

3.4.2. Exploring the unique two-stage fouling mechanism: interplay of organic scaffold formation and inorganic scaling. The two-stage fouling mechanism observed in AEMs during ED is a complex process influenced by the membrane's material properties, its interactions with organic and inorganic substances, and the specific operating conditions of the system.

In the first stage, the positively charged surface of the AEM, combined with its hydrophilic nature, creates an ideal environment for organic anions to adhere. AEMs are known to be particularly susceptible to organic foulants (*e.g.*, HA, carbohydrates, and aromatic compounds). This fouling primarily occurs on the membrane surface and within its internal structure owing to electrostatic, van der Waals, and hydrophobic interactions.[20] Therefore, these negatively charged organic compounds quickly accumulate on the membrane surface, forming an initial organic fouling layer. This layer creates a rough and uneven surface, which further promotes fouling by trapping additional contaminants.

As the organic layer thickens, it becomes a suitable foundation for inorganic deposition, particularly by divalent cations like calcium (Ca^{2+}). This transition marks the onset of the second fouling stage, characterized by the precipitation of salts such as calcium carbonate ($CaCO_3$). The presence of the organic layer facilitates the attachment and crystallization of inorganic salts, accelerating the fouling process and making it more severe over time.

The electric field in the ED system further intensifies this sequence by driving negatively charged particles toward the AEM, increasing their local concentration and enhancing the likelihood of fouling. Initially, organic fouling reduces membrane efficiency by obstructing ion transport. As inorganic scaling progresses, it exacerbates pore blockage, significantly impairing ion-exchange capacity.

This sequential fouling not only accelerates the deterioration of the membrane's physical structure but also compromises its selective permeability. As both organic and inorganic foulants accumulate, the cumulative impact accelerates membrane degradation, leading to a substantial decline in overall system performance.

3.5. Laboratory experiment *vs.* field application in ED membrane fouling

A pilot-scale ED unit was installed to evaluate their performance in treating groundwater with high hardness levels for a period of one year. Consistent with the laboratory findings depicted in Fig. 1, the water production rate achieved by the units was notable (refer to Fig. S10(a) and S10(b)). However, similar to the pattern observed in Fig. 1(b), the EC removal efficiency exhibited a sharp decline over time, despite an initially high performance (Fig. S10(b)). Post-operation analysis of the disassembled ED unit from Padaviya after one year of continuous operation revealed significant calcium scaling on the membranes (Fig. 7). This observation aligns with laboratory findings, where secondary fouling was predominantly attributed to the deposition of inorganic materials.

These findings highlight the urgency of developing effective cleaning strategies to mitigate fouling to establish ED as a sustainable water treatment solution for Sri Lanka. Although the water production rate remained largely unaffected, prolonged fouling progressively compromises water quality over time, underscoring the need for optimized maintenance protocols to sustain long-term ED performance.

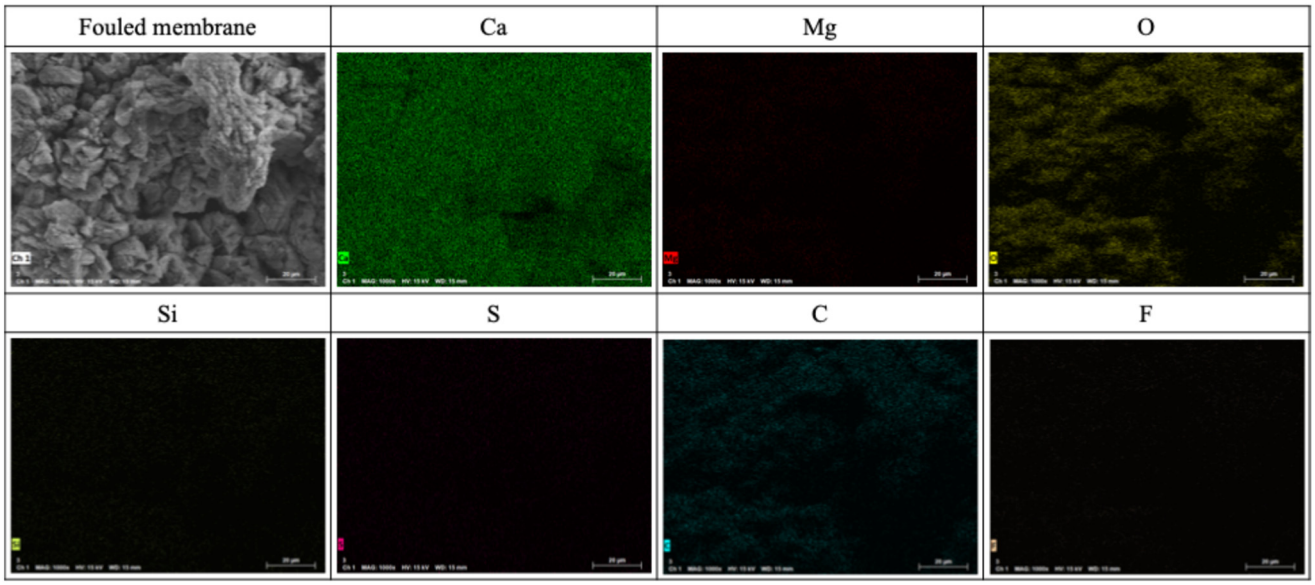

Fig. 7 EDS-mapping of fouled AEM after one year of operation in Sri Lanka.

3.6. Membrane characteristics under different cleaning methods

3.6.1. SEM analysis of fouling composition and efficacy of membrane cleaning strategies. Significant reduction of scaling was observed in all four cleaning strategies used in the study (Fig. 8). Distilled water was employed as a physical cleaning solution where all other three solutions were categorized under chemical cleaning reagents. The primary reactions involved in chemical cleaning include hydrolysis, saponification, solubilization, peptization, dispersion, and chelation.[24]

The scaling observed in the cleaned membrane, as shown by the high proportion of C, O, and Ca elements, suggests that $CaCO_3$ is the predominant component of fouling (Fig. S11–S14). This is observed in the cleaning methods of DW, NaOH, and HCl. However, it was observed that the peak height and area within the FTIR spectrum associated with $CaCO_3$ were comparatively smaller in cleaned membranes (Fig. S14), suggesting that the surface concentration of foulants was effectively lowered. The surfaces of the membranes exhibited a relatively clean appearance in all three reagents, with few variances. The surface morphology of the membrane surface subjected to DW cleaning (Fig. 8(a)) exhibited a noticeable improvement in smoothness. In conjunction with the obtained outcomes, DW partially mitigated scaling; however, a substantial amount remained. Membranes cleaned with NaOH showed evidence of remaining $CaCO_3$ crystals on the surface. This is likely because NaOH is effective at removing organic debris[25] but less effective at solubilizing inorganic scale. Enhanced elimination of inorganic foulants can be attained through the application of acidic agents due to the solubilization and chelation reaction that occurs between inorganic ions and acids.[24,26] As a result, the presence of the inorganic foulant on the membrane was effectively eliminated with the use of HCl solution.

However, despite the effectiveness of the cleaning process for HAc, the distinctive peaks associated with $CaCO_3$ in FTIR analysis[27–29] and the presence of Ca patches in EDS mapping were hardly distinguishable in the HAc-cleaned membrane (Fig. S14). However, the production of a gel layer (Fig. 8(d)) was detected during the HAc process, which was also noted by Wang S. *et al.* (2023)[27] in their research on the VMD desalination process. Even though the Ca and Mg fouling were not evident on the membrane after it had been cleaned

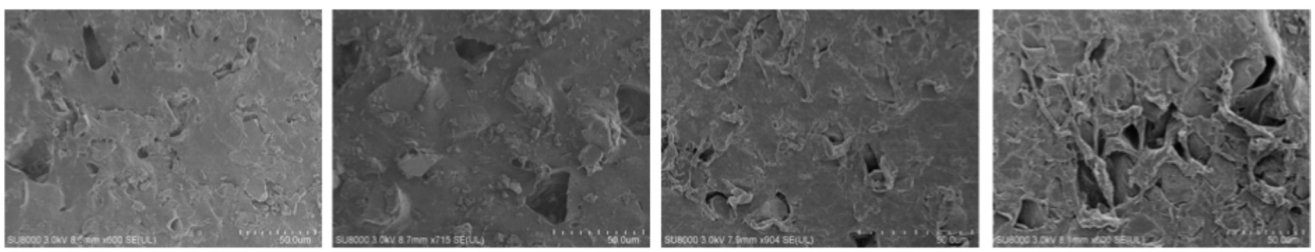

Fig. 8 Representative scanning electron microscopy (SEM) images of membrane after cleaning under (a) DW, (b) NaOH, (c) HCl and (d) citric acid.

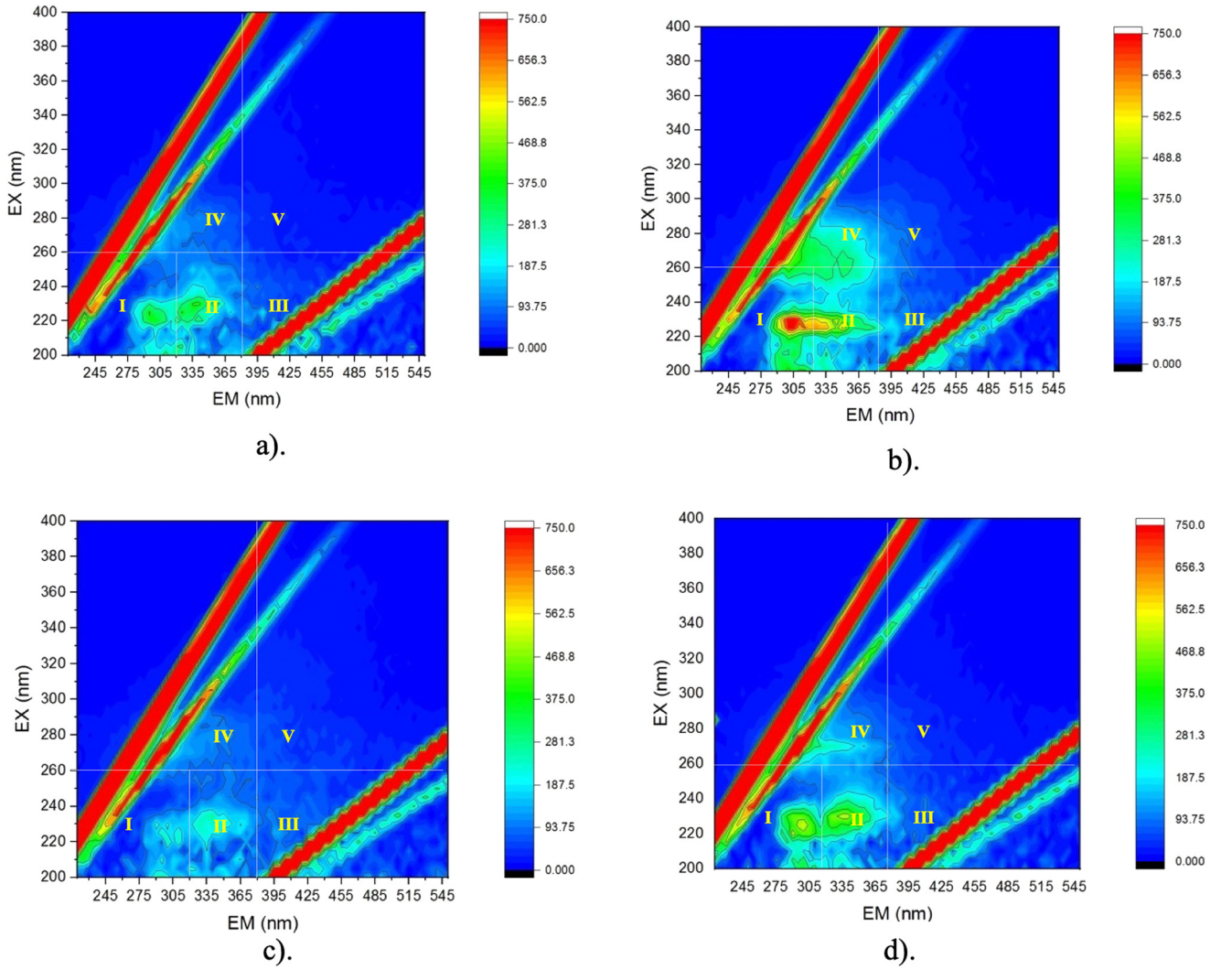

Fig. 9 Fluorescence excitation and emission matrix of the membrane cleaning solutions: (a) DW, (b) NaOH, (c) HCl and (d) citric acid for AEM.

with HAc, significant organic fouling was still found, implying that organic fouling formed first and could not be fully removed by acidic cleaning alone.

3.6.2. Three-dimensional fluorescence excitation–emission matrix analysis (3D-EEM). The effectiveness of membrane cleaning was assessed using 3D-EEM fluorescence spectroscopy, which provided insight into the removal patterns of organic compounds across different cleaning solutions applied to the AEM. Fig. 9 presents the fluorescence excitation and emission matrices of the cleaning solutions (a) distilled water (DW), (b) NaOH, (c) HCl, and (d) citric acid, highlighting the variations in compound removal efficiency.

Cleaning with deionized water (DW) revealed the presence of tyrosine-like aromatics (region I) and protein-like substances (region II), suggesting moderate removal efficiency while indicating that some organic matter remained on the membrane. In contrast, NaOH cleaning led to a significant reduction in these regions, highlighting its strong oxidative properties and effectiveness in mitigating biofouling, including the breakdown of high molecular weight humic substances. HCl cleaning had a slight effect on the reduction of aromatic proteins and lower molecular weight humic acids, suggesting its effectiveness in removing inorganic foulants rather than organic matter. Citric acid cleaning was highly effective, as evidenced by significant reductions in fluorescence intensity across regions associated with humic substances. This indicates that citric acid is particularly effective in dislodging complex fouling layers composed of both organic and inorganic components. Overall, the 3D-EEM spectroscopy analysis underscores the differential cleaning efficacy of each reagent, with citric acid emerging as the most efficient in removing both organic and inorganic contaminants from the AEM.

3.7. Cleaning strategies for field implementation

As discussed in section 3.4, the accumulation of organic and inorganic foulants on membranes occurs through distinct mechanisms, each contributing significantly to overall membrane fouling. Inorganic scaling is effectively addressed using acid-based cleaning, whereas organic fouling is

typically managed with alkaline cleaning agents like NaOH. However, a single cleaning solution is inadequate to address the complex fouling in brackish groundwater treatment in Sri Lanka (Fig. S16). Therefore, a two-step cleaning process is recommended: acidic solutions to remove inorganic fouling, followed by alkaline solutions to address organic fouling. A similar two-step cleaning approach was identified by An *et al.* (2023),[22] confirming its relevance to ED membrane fouling.

For professional users, a combination of HCl and NaOH is recommended for effective cleaning. These chemicals, commonly used in industrial-scale cleaning, should be handled exclusively by trained professionals following proper safety procedures. Post-chemical cleaning, membranes should be flushed with deionized water (DW) to remove residual contaminants. Although DW flushing effectively removes some foulants through hydraulic action, it is insufficient for insoluble scalants, highlighting the need for chemical cleaning.

For household or decentralized users, the use of HCl is discouraged due to potential health and handling risks. Instead, citric acid offers a safer and equally effective alternative for removing alkaline scaling. DW flushing remains a primary cleaning method for non-professionals, offering a safe way to maintain membranes without chemical exposure.

By adopting user-specific, two-step cleaning protocols, membrane performance can be effectively restored (Fig. S10(b)), ensuring the sustainable operation of ED systems for brackish groundwater treatment.

4. Conclusion

This study provides a comprehensive investigation into membrane fouling in ED systems used for brackish groundwater desalination, with a focus on elucidating fouling mechanisms and evaluating effective cleaning strategies. Through detailed membrane autopsies and statistical analysis, a two-stage fouling process was identified on AEMs. Initially, a compact organic fouling layer forms rapidly, followed by the development of alkaline scaling. The interaction between organic and inorganic foulants accelerates membrane degradation, compromising both the membrane's physical integrity and ion-selective permeability. This highlights the need for targeted fouling management strategies to mitigate the cumulative impact on membrane performance.

Our investigation into various cleaning methods revealed that physical cleaning techniques, such as DW and NaOH, were ineffective in removing alkaline scaling. In contrast, acidic solutions, particularly HCl and HAc, show promise in addressing inorganic scaling, with citric acid emerging as a viable option for household-level cleaning applications. Despite their respective strengths, none of the individual cleaning methods was able to fully eliminate all foulants. Based on these findings, we recommend a comprehensive cleaning protocol that combines acid cleaning followed by base cleaning to restore membrane performance and extend the operational lifespan of ED systems. This multi-step approach helps address both organic and inorganic fouling, improves membrane recovery and supports the long-term sustainability of brackish groundwater desalination systems.

Conflicts of interest

The authors declare no conflicts of interest.

Data availability

Supplementary information: this supplementary information (SI) file includes detailed water quality data, characterization of fouled membranes, field performance results, and cleaning strategy evaluations supporting the finding of this study. See DOI: **https://doi.org/10.1039/D5EW00498E**.

The data supporting this article have been included as part of the SI.

Acknowledgements

We gratefully acknowledge the China–Sri Lanka Joint Research and Demonstration Center for Water Technology, the China–Sri Lanka Joint Center for Education and Research, and the Department of National Community Water Supply for their essential support in facilitating field studies and providing technical assistance, which greatly contributed to the success of this research. This study was funded by the Program of China–Sri Lanka Joint Center for Education and Research, initiated by the Chinese Academy of Sciences, with additional financial support from The Belt and Road Master Fellowship Program (Grant No. 218611422020) and the ANSO Scholarship for Young Talents (Award Series No. 2021ANSOP123). We also extend our gratitude to the CAS President's International Fellowship Initiative (Project Number: 2024VEA0016) for supporting our co-author, R.M.G. Rajapakshe.

References

1 S. Indika, Y. Wei, T. Cooray, T. Ritigala, K. B. S. N. Jinadasa, S. K. Weragoda and R. Weerasooriya, Groundwater-Based Drinking Water Supply in Sri Lanka: Status and Perspectives, *Water*, 2022, **14**(9), 1428, DOI: **10.3390/w14091428**.

2 J. Ketharani, M. A. C. K. Hansima, S. Indika, D. R. Samarajeewa, M. Makehelwala, K. B. S. N. Jinadasa, S. K. Weragoda, R. M. L. D. Rathnayake, K. G. N. Nanayakkara, Y. Wei, S. L. Schensul and R. Weerasooriya, A Comparative Study of Community Reverse Osmosis and Nanofiltration Systems for Total Hardness Removal in Groundwater, *Groundw. Sustain. Dev.*, 2022, **18**(1), 100800, DOI: **10.1016/j.gsd.2022.100800**.

3 S. K. Patel, B. Lee, P. Westerhoff and M. Elimelech, The Potential of Electrodialysis as a Cost-Effective Alternative to Reverse Osmosis for Brackish Water Desalination, *Water Res.*, 2024, **250**, 121009, DOI: **10.1016/j.watres.2023.121009**.

4 I. C. Escobar, Chapter 14 Conclusion: A Summary of Challenges Still Facing Desalination and Water Reuse, *Sustainability Science and Engineering*, 2010, **2**, 389–397, DOI: **10.1016/S1871-2711(09)00214-1**.

5 M. A. C. K. Hansima, M. Makehelwala, K. B. S. N. Jinadasa, Y. Wei, K. G. N. Nanayakkara, A. C. Herath and R. Weerasooriya, Fouling of Ion Exchange Membranes Used in the Electrodialysis Reversal Advanced Water Treatment: A Review, *Chemosphere*, 2021, **263**, 127951, DOI: **10.1016/j.chemosphere.2020.127951**.

6 N. Pismenskaya, M. Bdiri, V. Sarapulova, A. Kozmai, J. Fouilloux, L. Baklouti, C. Larchet, E. Renard and L. Dammak, A Review on Ion-Exchange Membranes Fouling during Electrodialysis Process in Food Industry, Part 2: Influence on Transport Properties and Electrochemical Characteristics, Cleaning and Its Consequences, *Membranes*, 2021, **11**(11), 811, DOI: **10.3390/membranes11110811**.

7 L. Dammak, J. Fouilloux, M. Bdiri, C. Larchet, E. Renard, L. Baklouti, V. Sarapulova, A. Kozmai and N. Pismenskaya, A Review on Ion-Exchange Membrane Fouling during the Electrodialysis Process in the Food Industry, Part 1: Types, Effects, Characterization Methods, Fouling Mechanisms and Interactions, *Membranes*, 2021, **11**(10), 789, DOI: **10.3390/membranes11100789**.

8 Y. Lester, A. Hazut and A. Spanier, Formation of Organic Fouling during Membrane Desalination: The Effect of Divalent Cations and the Use of an Online Visual Monitoring Method, *Membranes*, 2022, **12**(12), 1177, DOI: **10.3390/membranes12121177**.

9 M. Freire-Gormaly and A. M. Bilton, Impact of Intermittent Operation on Reverse Osmosis Membrane Fouling for Brackish Groundwater Desalination Systems, *J. Membr. Sci.*, 2019, **583**, 220–230, DOI: **10.1016/j.memsci.2019.04.010**.

10 Y.-Q. Xu, X. Tong, Y.-H. Wu, H.-B. Wang, N. Ikuno and H.-Y. Hu, Comparison of the Reverse Osmosis Membrane Fouling Behaviors of Different Types of Water Samples by Modeling the Flux Change over Time, *Chemosphere*, 2022, **289**, 133217, DOI: **10.1016/j.chemosphere.2021.133217**.

11 X. Guo, C. Liu, B. Feng and Y. Hao, Evaluation of Membrane Fouling Control for Brackish Water Treatment Using a Modified Polyamide Composite Nanofiltration Membrane, *Membranes*, 2022, **13**(1), 38, DOI: **10.3390/membranes13010038**.

12 A. S. Gorzalski and O. Coronell, Fouling of Nanofiltration Membranes in Full- and Bench-Scale Systems Treating Groundwater Containing Silica, *J. Membr. Sci.*, 2014, **468**, 349–359, DOI: **10.1016/j.memsci.2014.06.013**.

13 S. Boivin and T. Fujioka, Membrane Fouling Control and Contaminant Removal during Direct Nanofiltration of Surface Water, *Desalination*, 2024, **581**, 117607, DOI: **10.1016/j.desal.2024.117607**.

14 T. P. Malalagama, Y. Fan, T. Binghui, L. H. Fei and Y. Min, Studying the Applicability of Electrodialysis Technology to Treat Groundwater in CKDu Regions, Sri Lanka: Operational Parameter Optimization of the Pilot Project, *IWA Water Supply*, 2024, **24**(9), 3077–3092, DOI: **10.2166/ws.2024.186**.

15 W. Lin, M. Li, K. Xiao and X. Huang, The Role Shifting of Organic, Inorganic and Biological Foulants along Different Positions of a Two-Stage Nanofiltration Process, *J. Membr. Sci.*, 2020, **602**, 117979, DOI: **10.1016/j.memsci.2020.117979**.

16 W. Xiang, M. Han, T. Dong, J. Yao and L. Han, Fouling Dynamics of Anion Polyacrylamide on Anion Exchange Membrane in Electrodialysis, *Desalination*, 2021, **507**, 115036, DOI: **10.1016/j.desal.2021.115036**.

17 W. Zhang, S. Yu, H. Zhao, X. Ji and R. Ning, Vacuum Membrane Distillation for Seawater Concentrate Treatment Coupled with Microbubble Aeration Cleaning to Alleviate Membrane Fouling, *Sep. Purif. Technol.*, 2022, **290**, 120864, DOI: **10.1016/j.seppur.2022.120864**.

18 Q. Xia, H. Guo, Y. Ye, S. Yu, L. Li, Q. Li and R. Zhang, Study on the Fouling Mechanism and Cleaning Method in the Treatment of Polymer Flooding Produced Water with Ion Exchange Membranes, *RSC Adv.*, 2018, **8**(52), 29947–29957, DOI: **10.1039/C8RA05575K**.

19 B. Vital, E. V. Torres, T. Sleutels, M. C. Gagliano, M. Saakes and H. V. M. Hamelers, Fouling Fractionation in Reverse Electrodialysis with Natural Feed Waters Demonstrates Dual Media Rapid Filtration as an Effective Pre-Treatment for Fresh Water, *Desalination*, 2021, **518**, 115277, DOI: **10.1016/j.desal.2021.115277**.

20 J. Choi, W.-S. Kim, H. K. Kim, S. C. Yang, J.-H. Han, Y. C. Jeung and N. J. Jeong, Fouling Behavior of Wavy-Patterned Pore-Filling Membranes in Reverse Electrodialysis under Natural Seawater and Sewage Effluents, *npj Clean Water*, 2022, **5**(1), 6, DOI: **10.1038/s41545-022-00149-2**.

21 Q. Xia, H. Guo, Y. Ye, S. Yu, L. Li, Q. Li and R. Zhang, Study on the Fouling Mechanism and Cleaning Method in the Treatment of Polymer Flooding Produced Water with Ion Exchange Membranes, *RSC Adv.*, 2018, **8**(52), 29947–29957, DOI: **10.1039/C8RA05575K**.

22 B. M. An, S. L. Aung, J. Choi, H. Cha, J. Cho, B. Byambaa and K. G. Song, Behavior of Solutes and Membrane Fouling in an Electrodialysis to Treat a Side-Stream: Migration of Ions, Dissolved Organics and Micropollutants, *Desalination*, 2023, **549**, 116361, DOI: **10.1016/j.desal.2022.116361**.

23 J. Liu, Y. Yu, S. Chen, H. Li, H. Zhang, J. Yao, S. Velizarov and L. Han, Electrochemical Analysis of Ion-Exchange Membranes Fouling during Electrodialysis Treatment of Real Shale Gas Flowback Water, *J. Membr. Sci.*, 2024, **706**, 122954, DOI: **10.1016/j.memsci.2024.122954**.

24 E. Zondervan and B. Roffel, Evaluation of Different Cleaning Agents Used for Cleaning Ultra Filtration Membranes Fouled by Surface Water, *J. Membr. Sci.*, 2007, **304**(1–2), 40–49, DOI: **10.1016/j.memsci.2007.06.041**.

25 Y. Meng, Q. Zhong, Y. Liu, Z. Yan, Y. Liang, H. Chang, H. Liang and R. D. Vidic, Evaluating Membrane Cleaning for Organic Fouling in Direct Contact Membrane Distillation, *J. Cleaner Prod.*, 2023, **410**, 137319, DOI: **10.1016/j.jclepro.2023.137319**.

26 A. Aguiar, L. Andrade, L. Grossi, W. Pires and M. Amaral, Acid Mine Drainage Treatment by Nanofiltration: A Study of Membrane Fouling, Chemical Cleaning, and Membrane Ageing, *Sep. Purif. Technol.*, 2018, **192**, 185–195, DOI: **10.1016/j.seppur.2017.09.043**.

27 S. Wang, Y. You, X. Wang, W. Huang, L. Zheng and F. Li, Fouling Mechanism and Effective Cleaning Strategies for

Vacuum Membrane Distillation in Brackish Water Treatment, *Desalination*, 2023, **565**, 116884, DOI: **10.1016/j.desal.2023.116884**.

28 M. Khanjani, D. J. Westenberg, A. Kumar and H. Ma, Tuning Polymorphs and Morphology of Microbially Induced Calcium Carbonate: Controlling Factors and Underlying Mechanisms, *ACS Omega*, 2021, **6**(18), 11988–12003, DOI: **10.1021/acsomega.1c00559**.

29 B. Purgstaller, V. Mavromatis, A. Immenhauser and M. Dietzel, Transformation of Mg-Bearing Amorphous Calcium Carbonate to Mg-Calcite – In Situ Monitoring, *Geochim. Cosmochim. Acta*, 2016, **174**, 180–195, DOI: **10.1016/j.gca.2015.10.030**.